Alfaro Eric (Orcid ID: 0000-0001-9278-5017)

Improved seasonal prediction skill of rainfall for the *Primera* season in Central America

Improved seasonal prediction skill of rainfall for the Primera season

Eric J. Alfaro[1,2,3,], Xandre Chourio[4], Ángel G. Muñoz[5,6], Simon J. Mason[6]*

1- Center for Geophysical Research, University of Costa Rica
2- School of Physics, University of Costa Rica
3- Center for Research in Marine Sciences and Limnology, University of Costa Rica
4- Observatorio Latinoamericano de Eventos Extraordinarios (OLE^2). Centro de Modelado Científico (CMC). Universidad del Zulia. Maracaibo. Venezuela.
5- Atmospheric and Oceanic Sciences (AOS). Princeton University. Princeton. USA.
6- International Research Institute for Climate and Society (IRI). The Earth Institute of Columbia University. New York. USA.
7-

*** Corresponding author address:**

Escuela de Fisica, 11501, 2060-Ciudad Universitaria Rodrigo Facio, Universidad de Costa

This is the author manuscript accepted for publication and has undergone full peer review but has not been through the copyediting, typesetting, pagination and proofreading process, which may lead to differences between this version and the Version of Record. Please cite this article as doi: 10.1002/joc.5366

Rica, San Jose, Costa Rica.

tel: +506 2511-5096**, fax:** +506 2234-2703**, email:** erick.alfaro@ucr.ac.cr

Abstract

This study explores the predictive skill of seasonal rainfall characteristics for the first rainy (and planting) season, May-June, in Central America. Statistical predictive models were built using a Model Output Statistics (MOS) technique based on canonical correlation analysis, in which variables forecast with the Climate Forecast System version 2 (CFSv2) were used as candidate predictors for the observed total precipitation, frequency of rainy days and mean number of extremely dry and wet events in the season. CFSv2 initializations from February to April were explored. The CFSv2 variables used in the study consist of rainfall, as in a typical MOS technique, and a combination of low-level winds and convective available potential energy (CAPE), a blend that has been previously shown to be a good predictor for convective activity. The highest predictive skill was found for the seasonal frequency of rainy days, followed by the mean frequency of dry events. In terms of candidate predictors, the zonal transport of CAPE (uCAPE) at 925 hPa offers higher skill across Central America than rainfall, which is attributed in part to the high model uncertainties associated with precipitation in the region. As expected, dynamical model predictors initialized in February provide lower skill than those initialized later. Nonetheless, the skill is comparable for March and April initializations. These results

suggest that the National Meteorological and Hydrological Services in Central America, and the Central American Regional Climate Outlook Forum, can produce earlier more skillful forecasts for May-June rainfall characteristics than previously stated.

KEYWORDS: SEASONAL CLIMATE PREDICTION, PRECIPITATION, CENTRAL AMERICA, STATISTICAL MODELS, MOS PREDICTIVE SCHEMES, CANONICAL CORRELATION ANALYSIS.

1. Introduction

Most of Central America has a bimodal mean annual precipitation pattern (Alfaro, 2002). The first peak of rainfall, which is associated with the first planting season or *Primera* (García-Solera and Ramírez, 2012), occurs during May-June, and a secondary rainfall maximum (usually larger in magnitude) in September-October. Both precipitation maxima are separated by a reduction in rainfall known as the midsummer-drought (MSD; Magaña *et al*., 1999; Karnauskas *et al*., 2013), known locally in Spanish as *veranillo* or *canícula*. This cycle implies mainly a combination of systems that involves the latitudinal migration of the Inter-Tropical Convergence Zone (ITCZ), the seasonal variation of solar radiation that influences latent heat flux, and low-level winds and their interactions with local orography. Some places in Central America, like the Caribbean coasts of Honduras, Costa Rica and Panama exhibit a different annual cycle: in these locations, precipitation tends to occur throughout the year, with peaks in July and December.

The most dominant climate driver in Central America is the North Atlantic Subtropical High (NASH; Taylor and Alfaro, 2005; Amador *et al*., 2006; Amador *et al*., 2016a) due to the strong easterly trades found on its equatorward flank. Coupled with a strong trade inversion, a cold ocean and reduced atmospheric humidity, the region is generally at its driest condition during the winter. With the onset of boreal spring, however, the subtropical high moves offshore and trade wind intensity decreases, with downstream convergence. The variation in the strength of the trades is an important determinant of climate throughout the year for Central America. During the onset of the rainy season there is also a weak trade inversion with altitude, the ocean warms and atmospheric moisture is abundant. The region is consequently at its wettest in the boreal late spring, during summer and early autumn seasons (Taylor and Alfaro, 2005). This relationship between the dominant precipitation annual cycle and the strength of the trade winds is presented in Fig. 1.

Fig. 1. around here.

Besides the NASH, other significant synoptic influences include (Alfaro *et al.*, 2016a): (a) the seasonal migration of the ITCZ – mainly affecting the Pacific side of southern Central America (Hidalgo *et al*., 2015); (b) the intrusions of polar fronts, originated at mid-latitudes, which modify the boreal dry winter and early spring climates of the northern Caribbean and north Central American regions (Zárate-Hernández, 2013); and (c) westward propagating tropical disturbances (Amador *et al*., 2010), which are a summer seasonal

feature associated with much rainfall, especially over the Caribbean region. The warm pools of the Americas constitute an important source of moisture for the North American Monsoon System (Wang and Enfield, 2001; 2003).

In Central America, Regional Climate Outlook Fora (RCOF) focus on the prediction of accumulated precipitation for the following target seasons: May-June-July (MJJ), August-September-October (ASO) and December-January-February-March (DJFM) (Donoso and Ramírez, 2001; García-Solera and Ramírez, 2012; Alfaro *et al.*, 2016b). Most of the seasonal outlooks presented in these fora follow a classical prediction scheme, in which, for example, observed SST fields are used to forecast rainfall for the subsequent target season.

Typically, these prediction schemes use statistical models based on canonical correlation analysis (CCA; Barnston and Ropelewski, 1992; Mason and Baddour, 2008; Navarra and Simoncini, 2010) to explore the predictability of seasonal rainfall in Central America, including MJJ (Alfaro, 2007; Fallas-López and Alfaro, 2012a; 2012b). For the early rainfall season (MJJ), positive and negative tropical Atlantic and Pacific SST anomalies, respectively, are associated with positive rainfall anomalies over a broad area located to the north of the studied region; and vice-versa. Cross-validated model results (Alfaro, 2007; Fallas-López and Alfaro, 2012a;b) show significant statistical predictive skill at seasonal scale over a large proportion of Central America. Nonetheless, using MJJ to define the *Primera* season has some disadvantages (Maldonado *et al.*, 2016a; Alfaro *et al.* 2016a).

During July, there is a strengthening of the trade winds and of the Caribbean Low-Level Jet (CLLJ; Amador, 2008), associated with the occurrence MSD in the Eastern Tropical Pacific (Herrera *et al.*, 2015, Maldonado *et al*., 2016b). Hence, July should be excluded in predictive studies of the first peak of the rainy season.

In this sense, Alfaro *et al.* (2016a) used gauge stations to build skillful canonical correlation analysis prediction models for the MJ (May-June) season as the first peak of the rainy season, using, as predictands, monthly rainfall accumulations and the Standardized Precipitation Index (SPI) over Central America. Two data sets were used as predictors: sea-surface temperature anomalies (SSTA) and the Palmer Drought Severity Index (PDSI) over the isthmus. CCA models using February´s SSTA and April´s PDSI showed significant skill values for the prediction of MJ accumulations and the SPI over a large proportion of Central America. The models´ canonical modes showed that warmer or cooler Eastern equatorial SSTAs in the Pacific, along with cooler or warmer SSTAs in the Tropical North Atlantic (TNA) during February, tend to be associated with drier or wetter conditions in almost all the isthmus during the following MJ season, respectively. The authors suggested that particular SST modes could modulate the MJ precipitation in Central America influencing the position of the ITCZ and the strength of the trade winds. Additionally, they concluded that drier or wetter soil moisture (PDSI) in April tends to be related with drier or wetter precipitation conditions in almost the entire isthmus during the following MJ season, respectively.

Maldonado *et al.* (2016a) also used CCA to explore the relationship between MJ precipitation anomalies during May to June in the Pacific slope of Central America, and SST fluctuations in the surrounding oceans. These authors studied variations in total precipitation, frequency of rainy days and the monthly occurrence of days with rainfall above and below the 80th and 20th percentile, respectively, due to changes in the nearby SSTs. In addition, they used a general circulation model forced with fixed SST to explore the sensitivity of the model to the SST patterns found using CCA. Their results showed that the SST over the tropical North Atlantic controls the precipitation fluctuations at inter-annual scales, due to its connection with the tropical upper tropospheric trough. Warmer temperatures result in SLP below normal in the Caribbean region, associated with an increase in the heights at 200 hPa. This vertical configuration reduces the wind shear between 850 and 200 hPa and increases the mid-level moisture convergence, creating enhanced conditions for deep convection, and favoring the generation of tropical cyclone activity. In the Pacific, a positive anomalous low-level moisture flux is observed from the ocean to the continental parts of the region, which may enhance the formation of mesoscale convective systems. The prediction schemes showed a lead-time of 1 or 2 months and can be used for operational climate services work. The atmospheric model output results of Maldonado et al. (2016a), replicate the main results found in the observed composite analysis, suggesting the potential use for Model Output Statistics (MOS) predictive schemes.

Our objective in this work is to explore the rainfall forecast skill of cross-validated CCA-based statistical models for *Primera* (MJ; Alfaro, 2002), while identifying additional candidate predictors to the more traditional observed SST fields already in use by the National Meteorological Services in the region.

A typical model output statistics (MOS) technique involves statistical corrections of dynamical model output or predictor, using observed data or predictand. For example, seasonal rainfall forecasts can be corrected using the observed rainfall for the same season and a CCA-based statistical model (e.g., Recalde-Coronel *et al*., 2014). Here, we first analyse the predictability of *Primera* following this same approach. Then we explore the suitability of a different predictor that has been used recently in Northern South America to forecast deep-convection activity (Muñoz *et al.,* 2016), involving a combination of both low-level winds and convective available potential energy (CAPE).

Outlooks of the *Primera* season are important because wetter (drier) MJ seasons tend to be associated with early (late) onsets of the rainy season (Alfaro *et al*., 2016a; Maldonado *et al*. 2016a). The early summer rainfall tends to be spatially heterogeneous across the Caribbean (Alfaro 2002; Jurya and Malmgren, 2012). So having a late start of the rains, like in 2015 (Amador *et al*., 2016b), followed by a significantly drier-than-normal season in MJ with a deep MSD in July and August (Alfaro, 2014; Hernandez and Fernandez, 2015; Solano, 2015; Maldonado *et al*. 2016b), could significantly affect key socioeconomic

sectors in Central America, as most cities in the isthmus are located on the Pacific slope.

After each Central American RCOF, Application Fora are held in the region with different socio-economic stakeholders, in order to "translate" the predictions to probable climate impacts for different sectors (Alfaro *et al*., 2016b; Maldonado *et al*., 2013; 2016a). Generally, these fora gather representatives of the Meteorological and Hydrological services, as well as members of the scientific and academic community, who work in conjunction with the stakeholders on the elaboration of regional and local climate impacts perspective for the next season. A clear outcome from the most recent meetings is the need to have predictions for extreme events like droughts and floods. Normally, time scales that are of concern to stakeholders are associated with the next outlook target season, meaning the next three or four months; it is of special interest to know if present conditions will persist or what kind of changes are expected. Those extreme events in Central America are influenced by inter-annual variability related to ENSO and decadal variability associated mainly with AMO and PDO (Maldonado *et al*., 2013; 2016a; 2016b); these candidate predictors were used by these authors to produce tailored seasonal forecasts using CCA.

2. Data

The statistical models used in this study involve two kinds of datasets: the variables to be forecast (predictands), and those variables used to forecast (predictors). Anomalies of these datasets were computed with respect to the 1982-2011 period.

2.1 Predictands

Four predictands representing different seasonal rainfall characteristics were selected: total precipitation, frequency of precipitation and average number of dry and extremely wet events. The details of how these variables were computed are presented in the Methodology section, but all are based on data from a total of 162 gauge stations with daily rainfall observations, provided by the different Meteorological Services in Central America. The location of each station is shown in Fig. 2. Since each meteorological station has different time coverage, a common time series length was selected according to the availability of data in the stations of Fig. 2: from January 1982 to December 2011 (30 years).

Fig. 2. around here

2.2 Predictors

In a typical MOS approach, rainfall output by a dynamical climate model is used as predictor for observed precipitation (e.g., Mason and Baddour, 2008; Recalde-Coronel *et al*., 2014).

The development of convective precipitation naturally depends on the presence of

environmental conditions favorable for the occurrence of deep convection (see Holton and Hakim, 2013, and references therein), and a particular index to measure the susceptibility to occurrence of deep convection is CAPE. This index provides a measure of the maximum possible kinetic energy that a statically unstable parcel can acquire (neglecting effects of water vapor and condensed water on the buoyancy), assuming that the parcel ascends without mixing with the environment and adjusts instantaneously to the local environmental pressure. Since most of the precipitation recorded in Central America is associated with deep convection of mesoscale systems, it is reasonable to consider CAPE in the present study.

Furthermore, as mentioned above, the CLLJ and trade winds are drivers controlling rainfall in the region, modifying circulation and moisture transport patterns, especially impacting low-level (925 hPa) zonal winds; hence, the latter should also be considered as a candidate predictor for precipitation in Central America (and the Caribbean).

As mentioned in the Introduction, a combination of low-level winds and CAPE has been shown to provide skillful forecasts of lightning activity, a known proxy for deep convection in the Tropics (Muñoz *et al.*, 2016). In northern South America, this compound candidate predictor provides higher skill than either of the component variables considered individually, and it also outperforms other traditional predictors like sea-surface temperature. This result is attributed to the fact that the combination is sensitive to changes

in the low-level atmospheric circulation associated with both large-scale and local drivers controlling precipitation, like El Niño-Southern Oscillation, the Atlantic Meridional Mode, the Inter-Tropical Convergence Zone migrations, the CLLJ and tropical cyclone activity (Muñoz *et al.*, 2016). Following these ideas, and because of the prevailing zonal component in the low-level winds of the region, we selected the zonal transport of CAPE at 925 hPa, or uCAPE, as the other candidate predictor for our study. This choice is also physically meaningful. The general transport of CAPE can be written, via the corresponding advection-diffusion equation, as

$$\nabla \cdot (\vec{v}CAPE) = \nabla \cdot (\kappa \nabla CAPE) - \frac{\partial CAPE}{\partial t} + SS, \quad (1)$$

where the first term on the right hand is the diffusion term (κ is the diffusivity), the second one is the temporal evolution of CAPE, and *SS* represents sink and source terms.

The Climate Forecast System version 2 (CFSv2; Saha and Tripp, 2011; Saha *et al*., 2014) was selected as the coupled ocean-atmosphere model to use, due to the availability of rainfall (referred to hereafter as PRECIP), 925 hPa winds and CAPE hindcasts for the period of interest, 1982-2011. The horizontal resolution for all candidate predictors is $1^o \times 1^o$. Considering always MJ as the target season, the February to April initialization times were explored, considering a total of 24 members for the calculation of the ensemble mean of uCAPE and PRECIP.

Different spatial domains were explored to adequately include spatial patterns of the predictors that maximized skill. The final spatial domain selected for PRECIP is defined by the box with coordinates 123°W - 49°W in longitude and 6°S - 34°N in latitude, while the box defined by the coordinates 120.5°W - 46.5°W in longitude and 6°S - 25°N in latitude was chosen as the best spatial domain for uCAPE. All hindcasts are available via the International Research Institute for Climate and Society (IRI) Data Library: http://iridl.ldeo.columbia.edu/expert/SOURCES/.NOAA/.NCEP/.EMC/.CFSv2/

2.3 Climate indices

The Niño3.4 index (Trenberth, 1997) was obtained from the National Oceanic and Atmospheric Administration (NOAA, http://www.cpc.ncep.noaa.gov/data/indices/sstoi.indices). The AMO (Enfield *et al*., 2001) index was also downloaded from the NOAA site (http://www.esrl.noaa.gov/psd/data/correlation/amon.us.long.data).

We also used horizontal wind data at 925 hPa, provided by the National Center for Environmental Prediction (NCEP) and National Center for Atmospheric Research (NCAR) reanalysis version 2 (Kistler et al. 2001), which has a horizontal resolution of 2.5° × 2.5°. The wind data are used to calculate the CLLJ magnitude index as in Amador (2008) and Amador *et al*. (2010).

3. Methodology

First, the gaps in the daily rain gauge time series were filled using the methodology described in Alfaro and Soley (2009), which combines autoregressive models and empirical orthogonal function (EOF) methods. From these time series, we estimated four predictands for every station to describe the amount and the temporal distribution of rainfall during May-June (MJ), using the same approach described by Maldonado *et al.* (2013). The first predictand represents the total precipitation (TP), the second corresponds to the frequency of rainy days or events (FRD), and the last two to the MJ average number of precipitation events exceeding the May and June 80th-percentile (p80) and under the May and June 20th-percentile (p20), representing wet extremes and the driest days, respectively.

The MOS methodology based on CCA (Mason and Baddour, 2008; Navarra and Simoncini, 2010) is the same one implemented by the Latin American Observatory (e.g., Recalde-Coronel *et al.*, 2014; Chourio, 2016) and can be summarized as follows. An EOF pre-filtering was applied to the CFSv2 rainfall and uCAPE fields (candidate predictors), and to TP, FRD, p20 and p80 fields (predictands) to reduce their dimensionality and to addresses the multiplicity errors (Mason and Baddour, 2008; Navarra and Simoncini, 2010). The maximum possible number of CCA modes is determined by the minimum number of EOFs between both fields. A maximum of 8 EOFs and CCA modes in the filtering stage was allowed. The CCA modes maximize the correlation between linear

combinations of the predictor's EOFs and linear combinations of the predictand's EOFs. Multiple CCA models were produced this way, one per each possible combination of the actual number of EOFs used for the predictor and the predictand. The maximum number of CCA modes is found for the best model fit. For each model, the spatially-averaged Kendall s Ärank correlation coefficient (or goodness index; Wilks, 2011) between the observed and forecast rainfall was computed using a 5-year cross-validation window. The optimal model was identified as the one having the maximum goodness index; the other models were discarded.

The MOS approach was applied to a total of 24 predictor-predictand configurations (4 predictands × 2 predictors × 3 initialization times per predictor). For the best 24 models the two-alternative forced-choice score (2AFC; Mason and Weigel, 2009), also known as generalized relative operating characteristics (GROC), was computed; the results were saved as spatial maps to evaluate the places with better skill for each one of the experiments. The 2AFC score measures discrimination, or how well a forecast system can distinguish between categories; e.g., below-normal rainfall from normal rainfall. It is related to the Kendall s Äused here to select the best CCA model. The expected 2AFC score for unskilled forecasts is 50%.

All the calculations were performed using the batch version of the Climate Predictability Tool (CPT) version 15.3.7, a software tool built and maintained by the International

Research Institute for Climate and Society (Mason and Tippett, 2016). CPT was chosen because it is actually in use for operational seasonal climate prediction in Central America; the batch version permitted to automate the execution of the tool for all the experiments and their different original variations in an organized and expedited way. The Latin American Observatory's *Datoteca* (Muñoz *et al.*, 2010; 2012; Chourio, 2016) was used to visualize the CPT output. The CCA models are publicly available on *Datoteca* in the following site: http://datoteca.ole2.org/maproom/DATOTECA-CONSTRUCCION/Paper-CA-Map-1/ .

The Spearman ranked correlations (Wilks, 2011) between the predictors' first CCA mode and the values of the climate indices mentioned in Section 2.3 for the same MJ season were calculated to explore potential relationships between the CCA modes and known climate variability modes. For those correlations were calculated the 95% bootstrap confidence intervals using 100000 simulations.

4. Results and Discussion

The spatial distribution of the MJ precipitation is presented in Fig. 3. Drier regions are observed in northern Belize and Guatemala, Central Guatemala, Honduras and Nicaragua, as well as in the Gulf of Panamá. The wettest regions are located along the Caribbean coast of Nicaragua and Costa Rica; Costa Rica also exhibits important rainfall totals along the southern central Pacific coast that extends through western Panama.

Fig. 3. around here

4.1 Model skill

The overall skill for the different models and initialization times (February to April) are summarized in Table 1. The CCA models are defined by the number of predictor-predictand-CCA modes that provide the best area-averaged Kendall s Äfor the MJ season, using MJ hindcasts of uCAPE (Table 1a) and PRECIP (Table 1b) as predictors. In general, the skill is very similar for March and April initializations, independently of the predictor chosen. A lead time represents a significant advantage for operational forecasts in the region, because climate services could be provided about two months before the target season. Furthermore, in March and April initializations, skill tends to be better for uCAPE than for PRECIP. Additional results for the models initialized in March are included in the Supplementary Material.

In order to analyse the spatial variability of skill, Fig. 4 shows the geographical distribution of 2AFC scores using uCAPE and PRECIP MJ hindcasts as predictor fields, initialized in April. In general, FRD and P20 are the predictands with highest skill across the isthmus; it is common to find that both statistical and dynamical models are better forecasting none or little rainfall (P20) than wetter rainfall events, and seasonal frequency tends to be more predictable than seasonal amounts or intensities (e.g., Moron *et al*., 2007; Muñoz *et al.*,

2016).

The predictor uCAPE clearly have a propensity to provide better skill than PRECIP almost everywhere and for all the predictands (Fig. 4). On the other hand, using PRECIP as predictor favours skill along the Pacific coast of Central America, although forecasts are generally unskilled (2AFC <= 50%) in most of the stations for TP and especially for P80.

Fig. 4. around here

4.2 CCA loadings

Fig. 5 around here

In order to better understand the sources of the skill observed in Fig. 4, we analysed the leading CCA modes for each model. Fig. 5 shows the loadings of the first CCA modes for the best models using MJ uCAPE as predictor and TP, FRD, p20 and p80 as predictands (Table 1). A positive uCAPE spatial pattern covering most of Central America, the Caribbean and northwestern South America occurring simultaneously with two negative uCAPE patterns, one in the northeast and another to the south-southeast of the domain (Fig. 5a), is maximally correlated with positive anomalies of TP over almost all Central America (all stations with positive loadings in Fig. 5b), and a few locations with negative TP anomalies which lie mostly along the Caribbean slope of Costa Rica (see stations with negative loadings in Fig. 5b). The uCAPE patterns are a broadly similar for FRD: in this case, a negative uCAPE configuration over southern Central America and a positive pattern

located to the northeastern of the domain are maximally correlated with negative anomalies for the frequency of rainy events basically everywhere in Central America (Fig. 5c,d). The uCAPE spatial patterns of the first CCA mode for p20 and p80 (Fig. 5e,g) are more similar to the ones for TP (Fig. 5a) than the ones for FRD (Fig. 5c), with an inverse relationship for the case of the p20 (i.e., stronger positive uCAPE anomalies associated with negative rainfall anomalies; Fig. 5f), and a direct relationship for p80, as expected (Fig 5h). Due to the linear character of the method, the opposite of what has been described here, i.e., exchanging positives for negatives (and vice versa) in each sentence, is also true.

A possible interpretation for this rainfall-uCAPE relationship is that a weaker trade wind (positive anomalies in u) decreases the vertical wind shear over the isthmus and favours the development of deep convective systems (associated with positive CAPE anomalies), which in turn tend to produce above-normal rainy conditions over the region. We attribute the observed inverted signal along the Caribbean slope of Costa Rica and western Panama to the Föhn effect of the Central American mountain chain.

Moreover, zonal transport of CAPE from the Pacific can enhance precipitation on the Pacific slope of Central America, favouring more wet extreme events (the opposite for dry extremes). The winds involved in the uCAPE predictor could also induce inhibition of convective systems on the Caribbean slope via moisture divergence, thus reducing rain there.

In the best models using PRECIP as predictor (Table 1 and Fig. 6), TP, p20 and p80 have the same predictor pattern, which appears in Fig. 6 as a tripolar configuration with a positive structure homogeneously covering most of northern South America, Central America and the Caribbean, and two negative ones: one over the Gulf of Mexico and the western Caribbean, and another from coastal Ecuador to the Galapagos Islands (Fig. 6a,e,g). This particular pattern is associated with positive anomalies for TP and p80 for most of the isthmus (negative anomalies for the Caribbean side of Costa Rica and Panama), while negative anomalies for p20 almost everywhere in Central America (Fig. 6b,f,h). For FRD, the predictor's spatial pattern shows a relatively strong zonally-elongated dipole covering all of Central America (in negative loadings in Fig. 6c) and a section of the Eastern Pacific below 4^{o}N, roughly from coastal Ecuador to 102^{o} W (in positive loadings in Fig. 6c); as expected, almost all the stations under study show a direct correlation with the structure covering Central America, e.g., negative rainfall anomalies in the CFSv2 model are associated with negative anomalies in the frequency of rainy days in the observations (Fig. 6,d).

Fig. 6. around here

Overall, the analysis of Kendall s Ä(Table 1), 2AFC scores (Fig. 4) and correlations of the observed and modelled leading modes (Figs. 7 and 8) indicates that uCAPE is a better predictor than PRECIP, especially for those models initialized in April. We attribute this

fact to a better representation by dynamical models --and by the CFSv2 in particular-- of the wind field, compared to the rainfall field. Furthermore, although the calculation of CAPE in dynamical models generally involves some of the same parameterizations used to simulate precipitation (e.g., to include entrainment rates), both theory and dynamical model output suggest that CAPE has less uncertainties than rainfall, at least in the Tropics (Seeley and Romps, 2015). Thus, using uCAPE for the development of operational climate forecast involving rainfall characteristics in Central America, and probably in the Caribbean nations and neighbouring countries, offers advantages over more traditional predictors like SST and model precipitation, in particular higher local skill and lead-time than previously stated (e.g., Alfaro *et al.* 2016a; Maldonado *et al.*, 2016a).

4.3 Leading CCA modes and climate indices

Finally, we explored potential associations between the leading CCA modes described in the previous paragraphs and some standard climate modes. Table 2 shows the Spearman correlation values between the MJ uCAPE leading mode inter-annual time series from Fig. 7 (red lines) and several climate indices for the same season. For the leading PRECIP mode (Fig. 8, red lines), the only statistically significant correlation (0.32, p-value < 0.10) was found between the AMO and the leading modes of TP, p20 and p80. The predictant (green lines in Figs. 7 and 8) and predictor mode correlations are statistically significant. Table 2 also shows that, individually, the best correlations with the oceanic indices were obtained

between the leading CCA modes and AMO as in Maldonado *et al.* (2016a); however, almost all the correlations improve when the normalized difference between the AMO and Niño3.4 indices is used, consistent with the results of Alfaro *et al*. (2016). These correlations suggest that positive (negative) Niño3.4 SSTAs, along with negative (positive) AMO index values during MJ, tend to be related to drier (wetter) conditions in almost all the isthmus during the target season. Even better correlations were obtained when using the CLLJ index, in which weaker (stronger) low-level jet conditions were associated with wetter (drier) conditions over Central America, decreasing (increasing) the vertical wind shear. This suggest than a warmer (cooler) Atlantic condition, when compared with the Eastern Equatorial Pacific, is associated with weaker (stronger) trade winds and CLLJ across Central America. These conditions favour (inhibit) deep convection over the region (Enfield and Alfaro, 1999; Amador, 2008; Hidalgo *et al.*, 2015).

Fig 7. around here

Fig. 8. around here

5. Conclusions

Skilful and tailored seasonal forecast models for several rainfall characteristic indices of the *Primera* season, May – June (MJ), in Central America, can be built using canonical correlation analysis. The zonal transport of CAPE (uCAPE) at 925 hPa provides better

seasonal forecast skill than standard predictors already in use by National Meteorological Services in the region, such as observed SST fields. Because of the free and continuously updated availability of the predictor fields, these models could be used operationally in Central America by the Regional Climate Outlook Forums (RCOF), especially as an input for the target season that includes the first peak of the rainy season. Our approach has the novelty of using a MOS scheme for the first time in the region, and it focuses not only on the prediction of accumulated precipitation, but also on the frequency of rainy days and the occurrences of wet and dry extremes. These alternative forecast products could be considered by the RCOF Application Fora, working with different socio-economic stakeholders in order to facilitate the translation of climate predictions to probable climate impacts for different sectors.

Lead-time is an important consideration in the usability of forecasts: the results presented here demonstrate that forecasts made from March predictors have comparable skill levels to those from April (see Supplementary Material). This additional month lead implies a significant advantage for operational climate forecasts in the region, because the associated climate information could be developed earlier than it normally is without compromising quality.

Seasonal predictability in the models is associated with a positive relationship between uCAPE values and rainfall over almost all Central America. This association may involve

weaker trade winds, related with positive anomalies in u, causing decreases in the vertical wind shear over the isthmus, which favors the generation of deep convective systems, i.e., positive anomalies in CAPE. The net effect is an enhancement of rainy conditions over Central America meaning positive anomalies in precipitation. The opposite behaviour on the Caribbean slope of Costa Rica and western Panama could be associated with the Föhn effect of the mountain chain, since most of the humidity advected by this positive anomaly in u from the surrounding Eastern Tropical Pacific, precipitates normally on the windward Pacific slope, reaching the leeward Caribbean slope drier.

There are strong synchronous relationships between the leading mode of variability of uCAPE and various indices of climate variability including sea-surface temperatures and the Atlantic Multidecadal Oscillation (AMO). The relationship is particularly strong with the normalized difference between AMO and Niño3.4 (AMO - Niño3.4 in Table 2): positive or negative Niño3.4 SSTAs, along with negative or positive AMO SSTAs, are associated with drier or wetter conditions along almost all the isthmus during the target season. The relationship between the different climate indices and the Caribbean Low-Level Jet (CLLJ) is even stronger; weaker or stronger jet conditions are associated with wetter or drier conditions over Central America, decreasing or increasing the vertical wind shear. Hence, a warmer or cooler Atlantic condition, when compared with the Eastern Equatorial Pacific, is associated with weaker or stronger trade winds and CLLJ winds across Central America. These conditions favour or decrease deep convection activity over

the region.

In Central America and especially on the Pacific slope, deep convection during the rainy season is associated with the convergence of the weak trade winds from the North Atlantic Subtropical High with mesoscale circulations like sea- and mountain-valley breezes that advect warm moist air from the Pacific to inland. This situation is enhanced by the ITCZ northward migration during boreal spring, which locates near or over the Central American isthmus. Thus, skillful prediction is possible using predictors that measure the susceptibility to occurrence of deep convection, CAPE, in conjunction with others that measure the strength of the trade winds, u. Since most of the precipitation recorded in Central America is associated with deep convection of mesoscale systems, it is reasonable to consider the inclusion of uCAPE as a physically-based candidate predictor of convective precipitation in Central America.

These results suggest possible ways of improving on forecast information from the Central American RCOF (García-Solera and Ramírez, 2012; Alfaro *et al.*, 2016b) through: a) the generation of rainfall consensus maps that give more specific weight to objective tools like IRI's CPT; b) the consideration of other predictor fields, like uCAPE in a MOS scheme to improve the skill in those regions in which SST fields have low skill or in climate seasons in which SSTs are in neutral conditions, like the case of the recent MJ 2017; and c) the development of new products related to extreme wet or dry event along with the frequency

of rainy days. These types of information are deemed very useful by the stakeholders to analyse probable impacts associated with the seasonal-scale climate hazards.

Acknowledgments

Alfaro would like to recognize the partial support of the following projects during this research: V.I. 805-B6-143 & 805-B7-507 (UCR, CONICIT-MICITT), B7-286 (UCREA), B4-227, B3-600, B0-065 and A9-532. To the Central American National Weather and Hydrology Services that provided the rainfall data used in this work. Muñoz was funded by the National Oceanic and Atmospheric Administration (NOAA) Oceanic and Atmospheric Research (OAR), under the auspices of the National Earth System Prediction Capability. The authors acknowledge the use of the Latin American Observatory's Datoteca (http://datoteca.ole2.org) and IRI's Data Library (http://iridl.ldeo.columbia.edu). Chourio was funded by Centro de Modelado Científico (CMC). Mason was funded by grant/cooperative agreement NA13OAR4310184 from the U.S. National Oceanic and Atmospheric Administration (NOAA). The views expressed herein are those of the authors and do not necessarily reflect the views of NOAA or any of its sub-agencies.

Supporting information captions

Figure S1. Spatial distribution of the 2AFC (or GROC) score, using uCAPE (left column) and PRECIP (right column) as predictor fields for the different MJ predictands: a) TP, b) FRD, c) P20 and d) P80.

Target season: MJ; CFSv2's hindcasts initialized in March. Units in %.

Figure S2. Loadings for the first CCA mode, using uCAPE as predictor (a, c, e and g) of the different predictands: b) TP, d) FRD, f) p20 and i) p80. Target season: MJ; CFSv2's hindcasts initialized in March.

Figure S3. Loadings for the first CCA mode, using PRECIP as predictor (a, c, e and g) of the different predictands: b) TP, d) FRD, f) p20 and i) p80. Target season: MJ; CFSv2's hindcasts initialized in March.

Figure S4. Time scores of the leading modes for the models using uCAPE as predictor for a) TP, b) FRD, c) p20 and d) p80. Predictor scores appear in red, predictand scores in green. Pearson correlations for the CCA leading modes were 0.894, 0.893, 0.837 and 0.803, respectively, with an associated p-value < 0.01 in all cases. Target season: MJ; CFSv2's hindcasts initialized in March.

Figure S5. Time scores of the leading modes for the models using PRECIP as predictor for a) TP, b) FRD, c) p20 and d) p80. Predictor scores appear in red, predictand scores in green. Pearson correlations for the CCA leading modes in this case were 0.710, 0.866,

0.831 and 0.871, respectively, with an associated p-value < 0.01 in all cases. Target season: MJ; CFSv2's hindcasts initialized in March.

Table S1. Spearman correlation between the uCAPE predictor mode 1 annual time series from Fig. S4 (red lines) and several climate variability indices. In parenthesis are the 95% bootstrap confidence intervals, they are calculated using 100000 simulations. Target season: MJ; CFSv2's hindcasts initialized in March.

Table S2. Spearman correlation between the PRECIP predictor mode 1 annual time series from Fig. S5 (red lines) and several climate variability indices. In parenthesis are the 95% bootstrap confidence intervals, they are calculated using 100000 simulations. Target season: MJ; CFSv2's hindcasts initialized in March.

References

Alfaro EJ. 2002. Some characteristics of the annual precipitation cycle in Central America and their relationships with its surrounding tropical oceans. *Tópicos Meteorológicos y Oceanográficos* **9**: 88-103.

Alfaro EJ. 2007. Uso del análisis de correlación canónica para la predicción de la

precipitación pluvial en Centroamérica. *Revista Ingeniería y Competitividad* **9**(2): 33-48.

Alfaro EJ. 2014. Caracterización del "veranillo" en dos cuencas de la vertiente del Pacífico de Costa Rica, América Central. *Revista de Biología Tropical* **62**(Supplement 4): 1-15.

Alfaro EJ, Hidalgo H, Mora N. 2016a. Prediction of MJ rainfall season using CCA models. *Tópicos Meteorológicos y Oceanográficos* **15**(2): 5-19.

Alfaro EJ, Hidalgo H, Mora N, Pérez-Briceño P, Fallas B. 2016b. Assessment of Central America Regional Climate Outlook Forum maps, 1998-2013. *Tópicos Meteorológicos y Oceanográficos*. **15**(1): 37-52.

Alfaro EJ, Soley J. 2009. Descripción de dos métodos de rellenado de datos ausentes en series de tiempo meteorológicas. *Revista de Matemáticas: Teoría y Aplicaciones* **16**(1): 59-74.

Alfaro EJ, Soley J, Enfield D. 2003. Uso de una Tabla de Contingencia para Aplicaciones Climáticas (Use of a Contingency Table for Climatic Applications). ESPOL/ FUNDESPOL: Guayaquil, Ecuador.

Amador JA. 2008. The Intra-Americas Sea Low-level Jet, overview and future research. *Annals of the New York Academy of Science* **1146**: 153-188. doi:10.1196/annals.1446.012

Amador JA, Alfaro, EJ, Lizano O, Magaña V. 2006. Atmospheric forcing in the Eastern Tropical Pacific: A review. *Progress in Oceanography* **69**: 101-142.

Amador JA, Alfaro EJ, Rivera E, Calderón B. 2010. Climatic features and their relationship with Tropical Cyclones over the Intra-Americas Seas. *Hurricanes and Climate Change* **2**: 149-173. doi:10.1007/978-90-481-9510-79.

Amador JA, Durán-Quesada AM, Rivera ER, Mora G, Sáenz F, Calderón B, Mora N. 2016. The easternmost tropical Pacific. Part II: Seasonal and intraseasonal modes of atmospheric variability. *Revista de Biología Tropical* **64**(Supplement 1): S23-S57.

Amador JA, Hidalgo HG, Alfaro EJ, Durán AM, Calderón B, Vega C. 2016b. Central America. [In State of the Climate 2015], Accepted in *Bull. Amer. Met. Soc*., In press.

Barnston AG, Ropelewski CF. 1992. Prediction of ENSO Episodes Using Canonical Correlation Analysis. *J Clim*. **5**(11): 1316–45.

Chourio X. 2016. The Latin American Observatory's Datoteca. *Climate Service Partnership Newsletter* April: 6. p 6. Available at: http://www.climate-services.org/wp-content/uploads/2015/05/CSP-newsletter-April-2016-2.pdf

Dai A, Trenberth KE, Qian T. 2004. A Global Dataset of Palmer Drought Severity Index for 1870–2002: Relationship with Soil Moisture and Effects of Surface Warming. *Journal of Hydrometeorology* **5**(6), 1117-1130. doi:10.1175/jhm-386.1

Donoso M., Ramirez P. 2001. Latin America and the Caribbean: Report on the Climate Outlook Forums for Mesoamerica. In *Coping with the climate: A step Forward*, Workshop Report: A multi-stakeholder review of Regional Climate Outlook Forums, Pretoria, South Africa. pp. 16-20.

Enfield DB, Mestas-Nuñez AM, Mayer DA, Cid-Serrano L. 1999. How ubiquitous is the dipole relationship in tropical Atlantic sea surface temperatures? Journal of Geophysical Research: Oceans, **104**(C4): 7841-7848. doi:10.1029/1998jc900109

Enfield DB, Mestas-Nuñez AM, Trimble PJ. 2001. The Atlantic Multidecadal Oscillation and its relation to rainfall and river flows in the continental U.S. *Geophysical Research Letters* **28**(10): 2077-2080. doi:10.1029/2000gl012745

Fallas-López B, Alfaro EJ. 2012a. Uso de herramientas estadísticas para la predicción estacional del campo de precipitación en América Central como apoyo a los Foros Climáticos Regionales. 1: Análisis de tablas de contingencia. *Revista de Climatología* **12**: 61-79.

Fallas-López B, Alfaro EJ. 2012b. Uso de herramientas estadísticas para la predicción estacional del campo de precipitación en América Central como apoyo a los Foros Climáticos Regionales 2: Análisis de Correlación Canónica. *Revista de Climatología* **12**: 93-105.

García-Solera I, Ramirez P. 2012. Central America's Seasonal Climate Outlook Forum.

The Climate Services Partnership, 8 pp. Available at: http://www.climate-services.org/sites/default/files/CRRH_Case_Study.pdf (visited 16/01/2014).

Gershunov A, Barnett TP. 1998. Interdecadal Modulation of ENSO Teleconnections. *Bulletin of the American Meteorological Society* **79**(12): 2715-2725. doi:10.1175/1520-0477(1998)0792.0.co;2

Hartmann DL. 2015. Pacific sea surface temperature and the winter of 2014. *Geophysical Research Letters* **42**: 1894–1902. doi:10.1002/2015GL063083.

Hernández K, Fernández W. 2015. Estudio de la evaporación para el cálculo del inicio y la conclusión de la época seca y lluviosa en Costa Rica. *Tópicos Meteorológicos y Oceanográficos* **14**: 18–26.

Herrera E, Magaña V, Caetano E. 2015. Air-sea interactions and dynamical processes associated with the midsummer drought. *International Journal of Climatology* **35**: 1569–1578. doi:10.1002/joc.4077.

Hidalgo HG, Alfaro EJ, Quesada-Montano B. 2016. Observed (1970-1999) climate variability in Central America using a high-resolution meteorological dataset with potential for climate change studies. *Accepted in Climatic Change*.

Hidalgo HG, Durán-Quesada AM, Amador JA, Alfaro EJ. 2015. The Caribbean Low-Level Jet, the Inter-Tropical Convergence Zone and precipitation patterns in the Intra-Americas

Sea: A proposed dynamical mechanism. *Geografiska Annaler*, Series A, Physical Geography, **97**(1): 41-59. doi:10.1111/geoa.12085

Holton JR, Hakim GJ. 2013. *An Introduction to Dynamic Meteorology* (5th ed.). Waltham, MA: Academic Press.

Hurrell JW, Deser C. 2009. North Atlantic climate variability: The role of the North Atlantic Oscillation. *Journal of Marine Systems* **78**(1): 28-41. doi:10.1016/j.jmarsys.2008.11.026

Jury MR, Malmgren BA. 2012. Joint modes of climate variability across the inter-Americas. *International Journal of Climatology* **32**: 1033–1046. doi:10.1002/joc.2324

Kalnay E, Kanamitsu M, Kistler R, Collins W, Deaven D, Gandin L, Iredell M, Saha S, Joseph D. 1996. The NCEP/NCAR 40-Year Reanalysis Project. *Bulletin American Meteorological Society*, **77**: 437-471.

Karnauskas KB, Giannini A, Seager R, Busalacchi AJ. 2013. A simple mechanism for the climatological midsummer drought along the Pacific coast of Central America. *Atmósfera* **26**:261–281.

Kistler R, Collins W, Saha S, White G, Woollen J, Kalnay E, Chelliah M, Ebisuzaki W, Kanamitsu M, Kousky V, van den Dool H, Jenne R, Fiorino M. 2001. The NCEP-NCAR 50-Year Reanalysis: Monthly Means CD-ROM and Documentation. *Bulletin American*

Meteorological Society, **82**: 247–267. doi:10.1175/1520-0477(2001)082<0247:TNNYRM>2.3.CO;2.

Magaña VO, Amador JA, Medina S. (1999). The mid-summer drought over Mexico and Central America. *Journal of Climate*, **12**: 1577-1588.

Maldonado T, Alfaro EJ, Fallas B, Alvarado L. (2013). Seasonal prediction of extreme precipitation events and frequency of rainy days over Costa Rica, Central America, using Canonical Correlation Analysis. *Advances in Geosciences* **33**(33): 41-52.

Maldonado T, Alfaro EJ, Rutgersson A, Amador JA. 2016a. The early rainy season in Central America: the role of the tropical North Atlantic SSTs. *Int. J. Climatol*. doi:10.1002/joc.4958.

Maldonado T, Rutgersson A, Alfaro EJ, Amador J, Claremar B. 2016b. Interannual variability of the midsummer drought in Central America and the connection with sea surface temperatures. *Advances in Geosciences*, **42**: 35-50. doi:10.5194/adgeo-42-35-2016.

Mason SJ, Baddour O. 2008. Statistical modelling. In: Troccoli, A., Harrison, M., Anderson, D.L.T., Mason, S.J. (Eds.), *Seasonal Climate: Forecasting and Managing Risk*. Vol. 82 of Nato Science Series. IV: Earth and Environmental Sciences, Springer Netherlands, Dordrecht.

Mason SJ, Tippett MK. 2016. Climate Predictability Tool version 15.3, Columbia

University Academic Commons. http://dx.doi.org/10.7916/D8NS0TQ6.

Mason SJ, Weigel AP. 2009. A generic forecast verification framework for administrative purposes. *Mon. Wea. Rev.*, **137**: 331–349.

Moron V, Robertson AW, Ward MN, Camberlin P, 2007. Spatial coherence of tropical rainfall at the regional scale. *J. Clim*. **20**: 5244–5263. http://dx.doi.org/10.1175/2007JCLI1623.1.

Muñoz ÁG, López MP, Velásquez R et al. 2010. An environmental watch system for the Andean countries: El Observatorio Andino. *Bull. Amer. Meteor. Soc.* **91**: 1645–1652 http://dx.doi.org/10.1175/2010BAMS2958.1

Muñoz ÁG, Ruiz D, Ramírez P, León G, Quintana J, Bonilla A, Torres W, Pastén M, Sánchez O. 2012. *Risk Management at the Latin American Observatory*. In Risk Management — Current Issues and Challenges, N. Banaitiene, Ed., InTech. pp. 532–556.

Muñoz ÁG, Díaz-Lobatón J, Chourio X, Stock, MJ. 2016. Seasonal prediction of lightning activity in NorthWestern Venezuela: Large-scale versus local drivers. *Atmospheric Research*, **172–173**: 147–162.

Muñoz E, Wang C, Enfield D. 2010. The Intra-Americas Springtime Sea Surface Temperature Anomaly Dipole as Fingerprint of Remote Influences. *Journal of Climate*, **23**(1): 43-56. doi:10.1175/2009jcli3006.1

Navarra A, Simoncini V. 2010. *A Guide to Empirical Orthogonal Functions for Climate Data Analysis*. Springer. DOI 10.1007/978-90-481-3702-2 1

Recalde-Coronel GC, Barnston AG, Muñoz ÁG. 2014. Predictability of December–April Rainfall in Coastal and Andean Ecuador. *J Appl Meteorol Climatol*. 17;53(6):1471–93.

Saha S, Tripp P. 2011. CFSv2 retrospective forecasts. NOAA/NWS/NCEP Environmental Modeling Center Tech. Rep., 12 pp.

——, at al. 2014: The NCEP Climate Forecast System version 2. *J. Climate*, 27, 2185–2208, doi:10.1175/JCLI-D-12-00823.1.

Seeley JT, Romps DM. 2015. The Effect of Global Warming on Severe Thunderstorms in the United States. *J Clim*. **28**(6):2443–58.

Smith, T., Reynolds, R., Peterson, T. C., & Lawrimore, J. (2007). Improvements to NOAA's Historical Merged Land–Ocean Surface Temperature Analysis (1880–2006). Journal of Climate, 21, 2283 – 2296.

Solano E. 2015. Análisis del comportamiento de los períodos caniculares en Costa Rica en algunas cuencas del Pacífico Norte y del Valle Central entre los años 1981 y 2010. Tesis de Grado, Licenciatura, Escuela de Física, Universidad de Costa Rica, San José, Costa Rica.

Taylor M, Alfaro EJ. 2005. *Climate of Central America and the Caribbean*. In: Encyclopedia of World Climatology (pp 183-189), Springer, Netherlands.

Trenberth KE. 1997. The Definition of El Niño. *Bulletin of the American Meteorological Society*, **78**(12): 2771-2777. https://doi.org/10.1175/1520-0477(1997)078<2771:TDOENO>2.0.CO;2

Wang C, Enfield DB. 2001. The tropical western hemisphere warm pool. *Geophysical Research Letters*, **28**(8): 1635-1638.

Wang C, Enfield DB. 2003. A further study of the tropical western hemisphere warm pool. *Journal of Climate*, **16**: 1476-1493.

Webb RS, Rosenzweig CE., Levine ER. 1993. Specifying land surface characteristics in general circulation models: Soil profile data set and derived water-holding capacities. *Global Biogeochemical Cycles*, **7**(1): 97-108. doi:10.1029/92gb01822

Wilks DS. 2011. *Statistical Methods in the Atmospheric Sciences* (vol. 100). Academic Press.

WMO. 2012. *Standardized Precipitation Index User Guide* (M. Svoboda, M. Hayes and D. Wood). (WMO-No. 1090), Geneva.

Xue Y, Smith TM, Reynolds RW. 2003. Interdecadal Changes of 30-yr SST Normals during 1871–2000. *Journal of Climate* **16**(10): 1601-1612. doi:10.1175/1520-0442-16.10.1601

Zárate-Hernández E. 2013. Climatología de masas invernales de aire frío que alcanzan

Centroamérica y el Caribe y su relación con algunos índices Árticos. *Tópicos Meteorológicos y Oceanográficos*, **12**(1): 35-55.

Tables

Table 1. Modes of the optimal model (X, Y, CCA) and spatial average Kendall Ävalues for the MJ season for the different CCA models, using MJ a) uCAPE and b) PRECIP field as predictors, initialized from February to April.

a)	April		March		February	
	Modes	Ä	Modes	Ä	Modes	Ä
TP	8,5,2	0.14	8,6,1	0.16	3,8,1	0.04
FRD	8,3,3	0.22	7,6,3	0.23	5,2,1	0.09
p20	8,7,4	0.19	7,4,2	0.19	4,3,1	0.07
p80	7,6,3	0.11	8,1,1	0.13	3,3,1	0.03

b)	April		March		February	
	Modes	Ä	Modes	Ä	Modes	Ä
TP	1,1,1	0.12	5,1,1	0.13	6,8,2	0.09
FRD	3,3,3	0.16	7,1,1	0.21	5,8,1	0.12
p20	1,1,1	0.15	7,1,1	0.18	5,6,1	0.12
p80	1,1,1	0.08	7,5,1	0.10	6,7,1	0.10

Table 2. Spearman correlation between the uCAPE predictor mode 1 annual time series from Fig. 7 (red lines) and several climate variability indices. In parenthesis are the 95% bootstrap confidence intervals, they are calculated using 100000 simulations. Target season: MJ; CFSv2's hindcasts initialized in April. For details see main text.

	AMO	Niño 3.4	AMO-Niño 3.4	CLLJ
TP	0.40 [0.135, 0.647]	-0.33 [-0.550, -0.091]	0.46 [0.240, 0.667]	-0.47 [-0.644, -0.232]
FRD	0.37 [0.101, 0.615]	-0.27 [-0.484, -0.024]	0.38 [0.124, 0.620]	-0.18 [-0.393, 0.072]
p20	-0.34 [-0.579, -0.067]	0.02 [-0.236, 0.286]	-0.22 [-0.462, 0.046]	0.52 [0.303, 0.672]
p80	0.40 [0.133, 0.650]	-0.30 [-0.527, -0.062]	0.45 [0.213, 0.660]	-0.44 [-0.623, -0.202]

Figure legends

Figure 1. Annual cycle of the monthly mean a) accumulated precipitation and b) zonal wind

values recorded at Center for Geophysical Research - CIGEFI station (9.94ºN, 84.04ºW), Costa Rica. The Spearman correlation of the monthly time series from January 1995 to October 2016 is 0.72 with an associated p-value < 0.01.

Figure 2. Location of the rain gauge stations used (red dots).

Figure 3. Spatial distribution of average precipitation accumulates (1982-2011) using the stations plotted in Figure 2.

Figure 4. Spatial distribution of the 2AFC (or GROC) score, using uCAPE (left column) and precipitation (right column) as predictor fields for the different MJ predictands: TP (a,b), FRD (c,d), P20 (e,f) and P80 (g,h). Target season: MJ; CFSv2's hindcasts initialized in April. Units in %.

Figure 5. Loadings for the first CCA mode, using uCAPE as predictor (a, c, e and g) for the different predictands: b) TP, d) FRD, f) p20 and i) p80. Target season: MJ; CFSv2's hindcasts initialized in April.

Figure 6. Loadings for the first CCA mode, using PRECIP as predictor (a, c, e and g) for the different predictands: b) TP, d) FRD, f) p20 and i) p80. Target season: MJ; CFSv2's hindcasts initialized in April.

Figure 7. Time scores of the leading modes for the models using uCAPE as predictor for a) TP, b) FRD, c) p20 and d) p80. Predictor scores appear in red, predictand scores in green.

Pearson correlations for the CCA leading modes were 0.841, 0.860, 0.901 and 0.827, respectively, with an associated p-value < 0.01 in all cases. Target season: MJ; CFSv2's hindcasts initialized in April.

Figure 8. Time scores of the leading modes for the models using PRECIP as predictor for a) TP, b) FRD, c) p20 and d) p80. Predictor scores appear in red, predictand scores in green. Pearson correlations for the CCA leading modes in this case were 0.39 (p-value < 0.05), 0.47 (p-value < 0.01), 0.31 (p-value < 0.10) and 0.68 (p-value < 0.01), respectively. Target season: MJ; CFSv2's hindcasts initialized in April.

a)

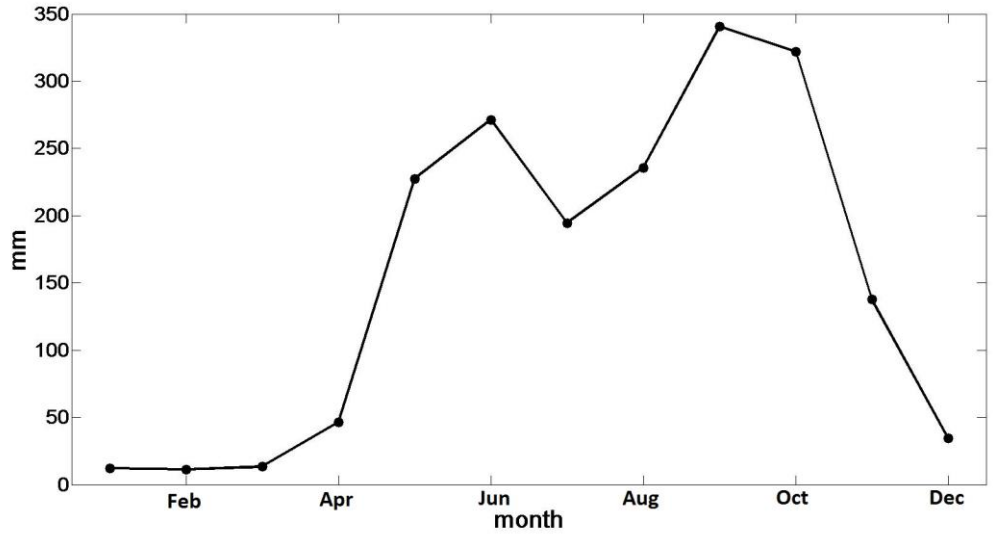

b)

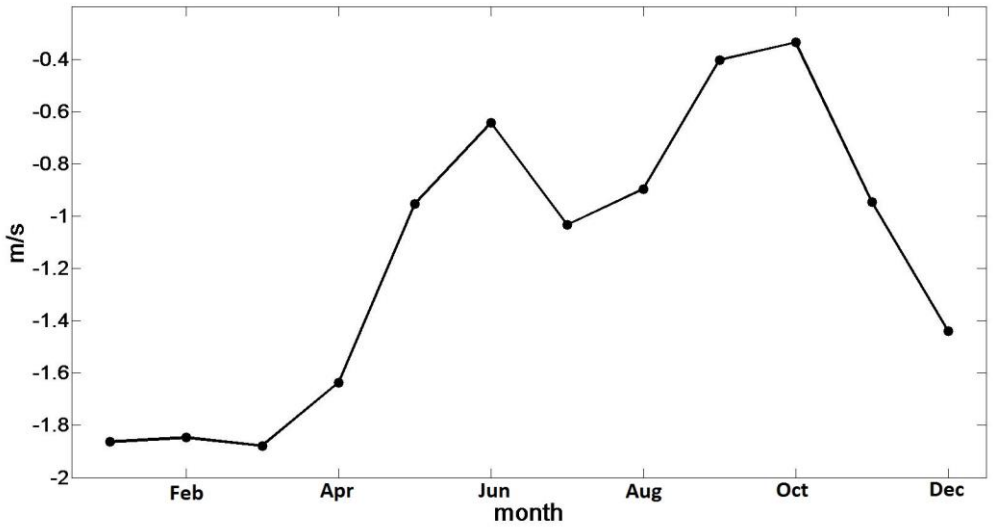

Fig. 1

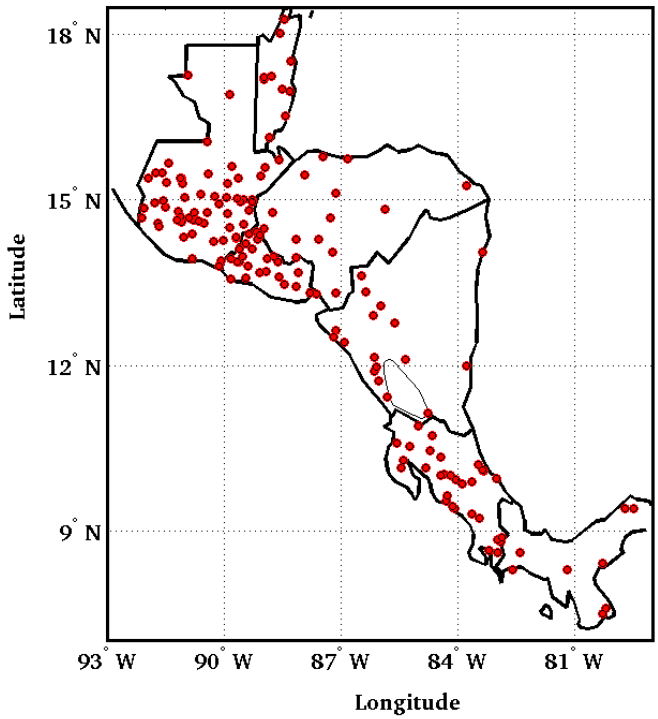

Fig 2.

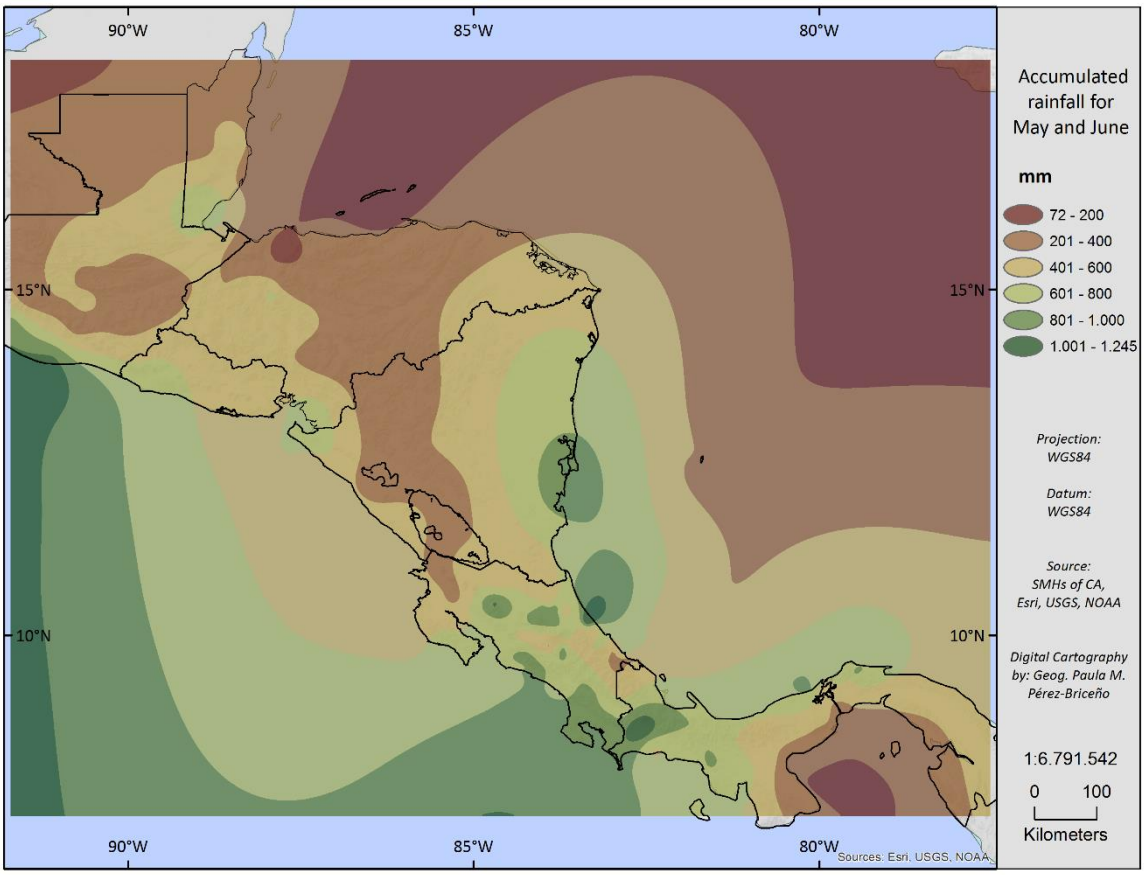

Fig 3.

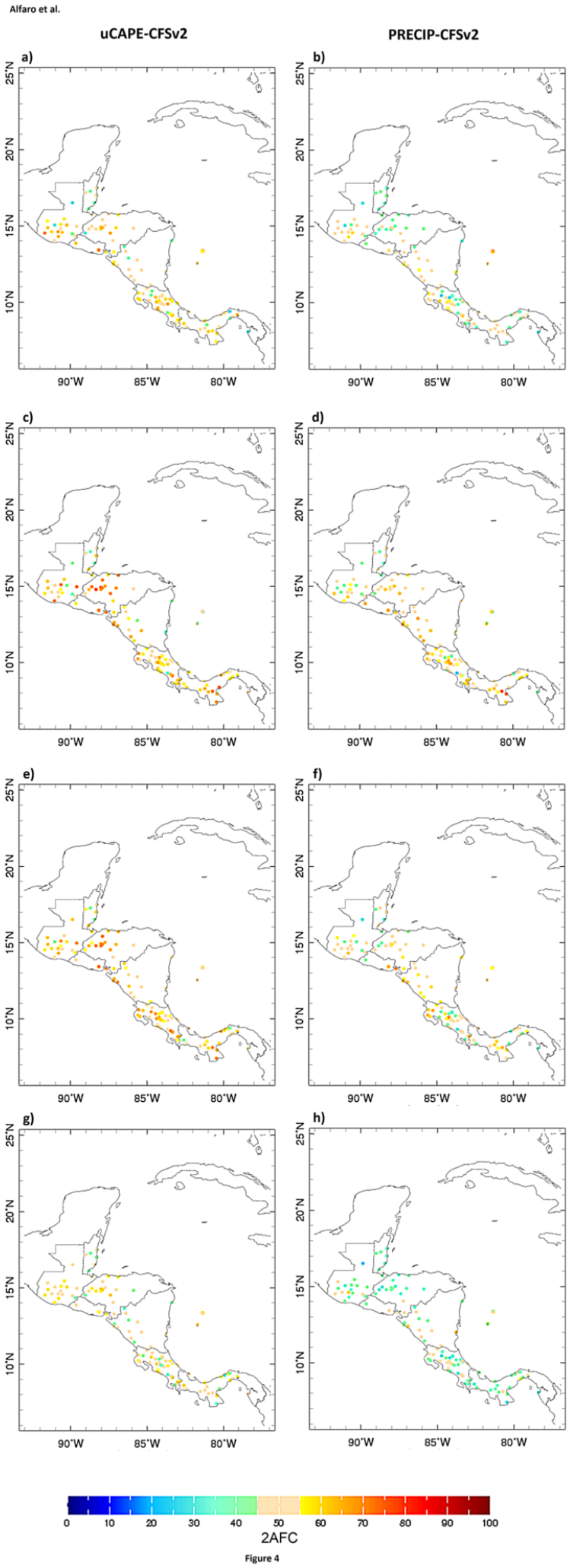

Figure4.tif

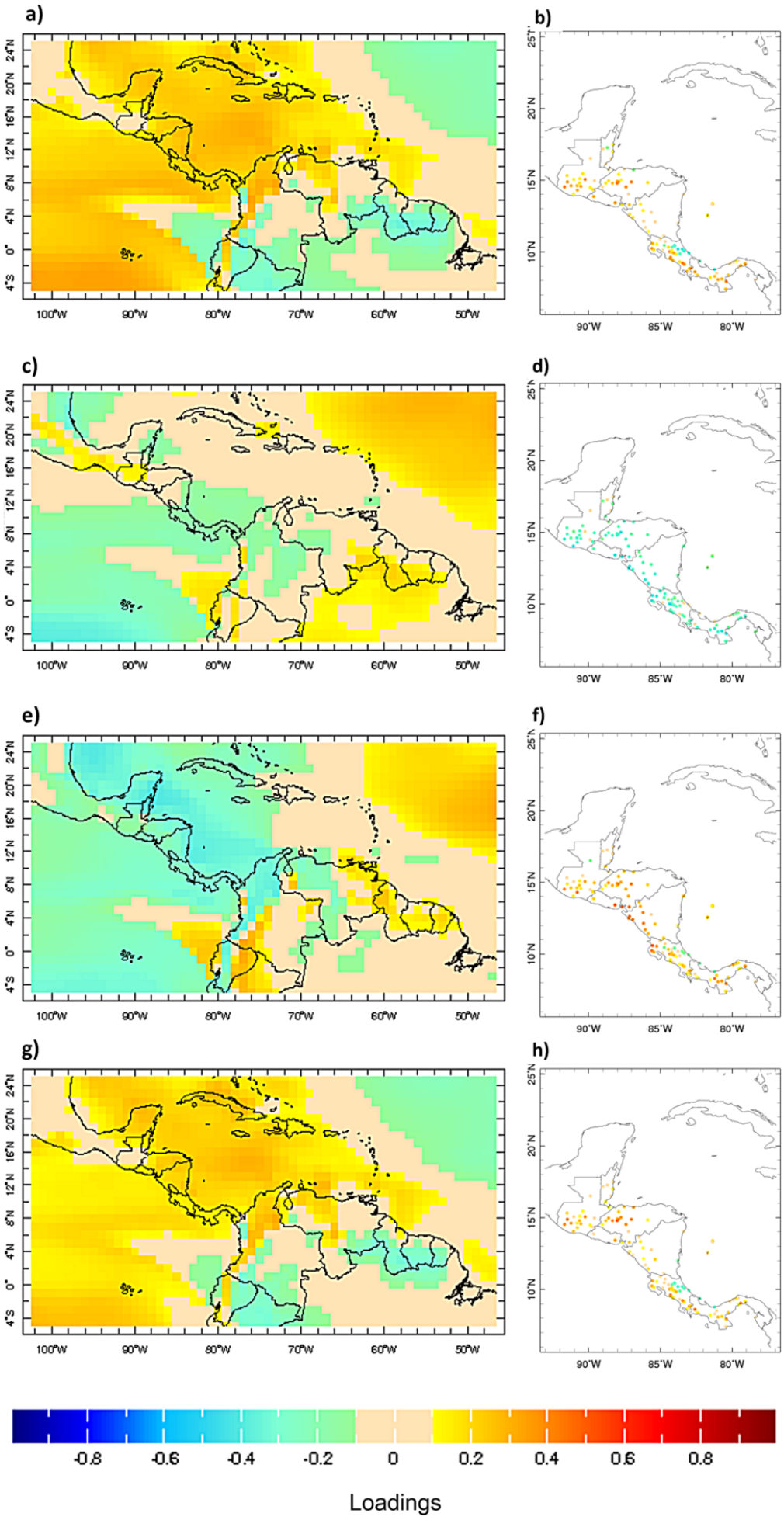

Figure 5

Figure5.tif

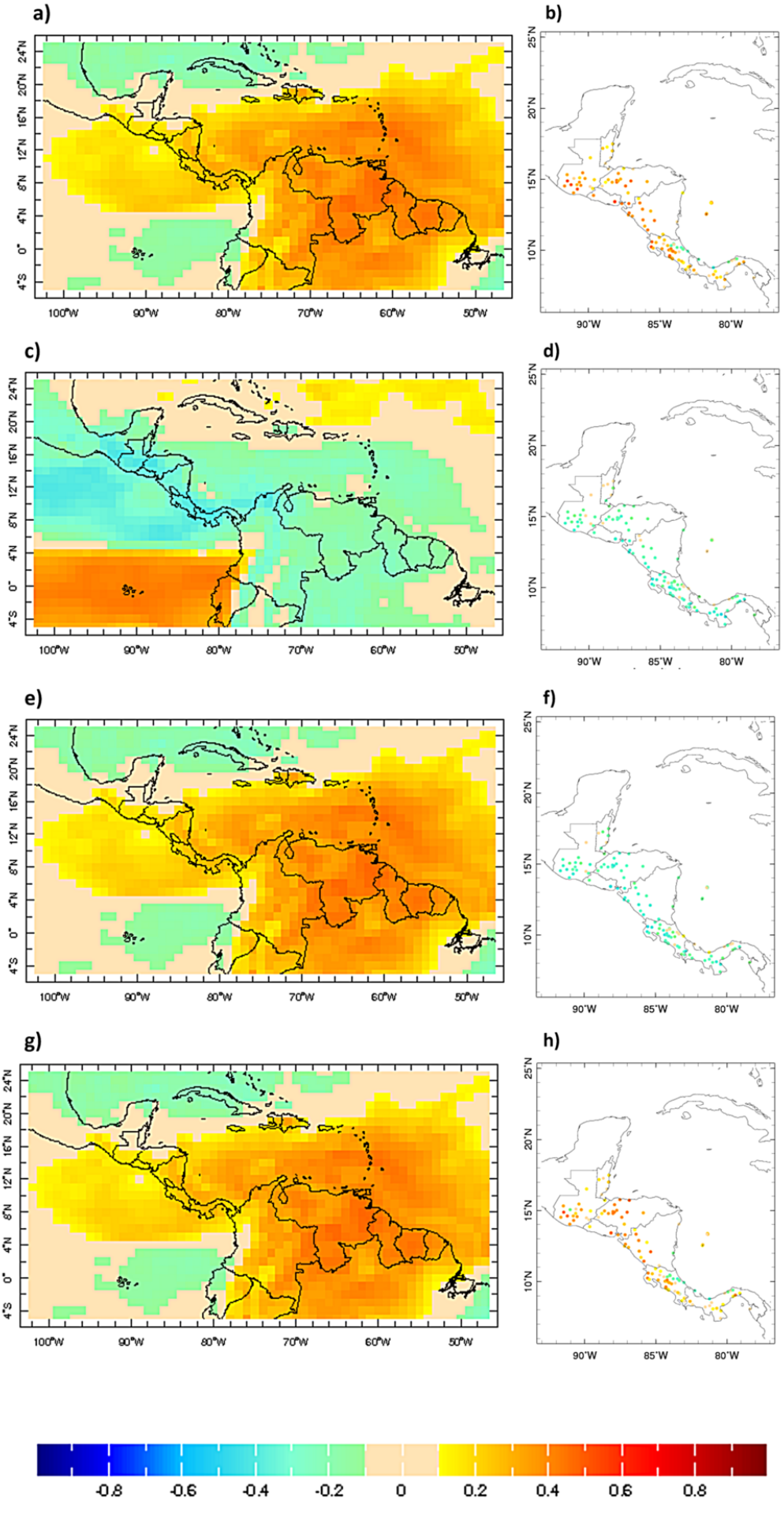

Figure 6

Figure6.tif

Fig. 7

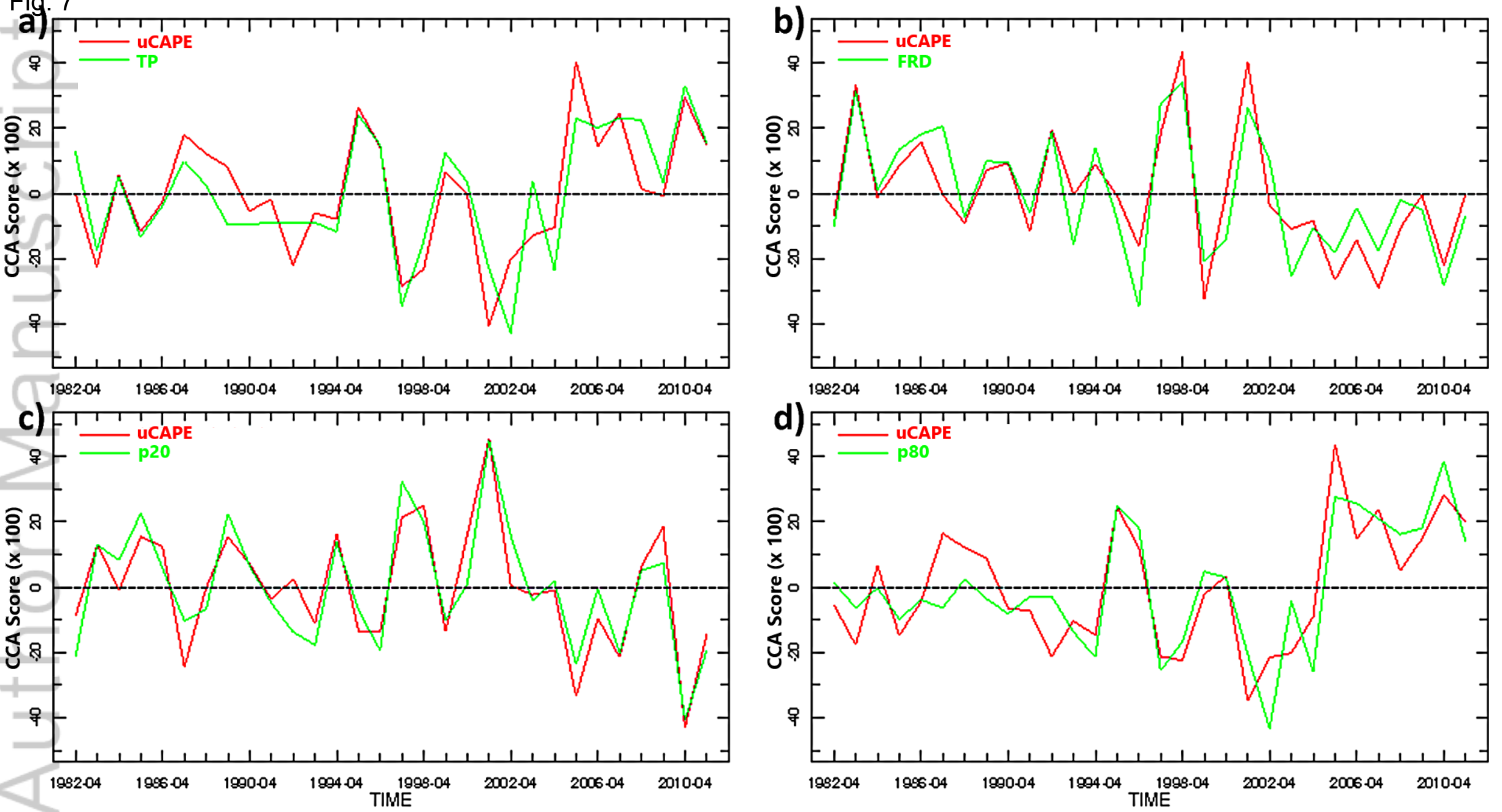

Fig. 8

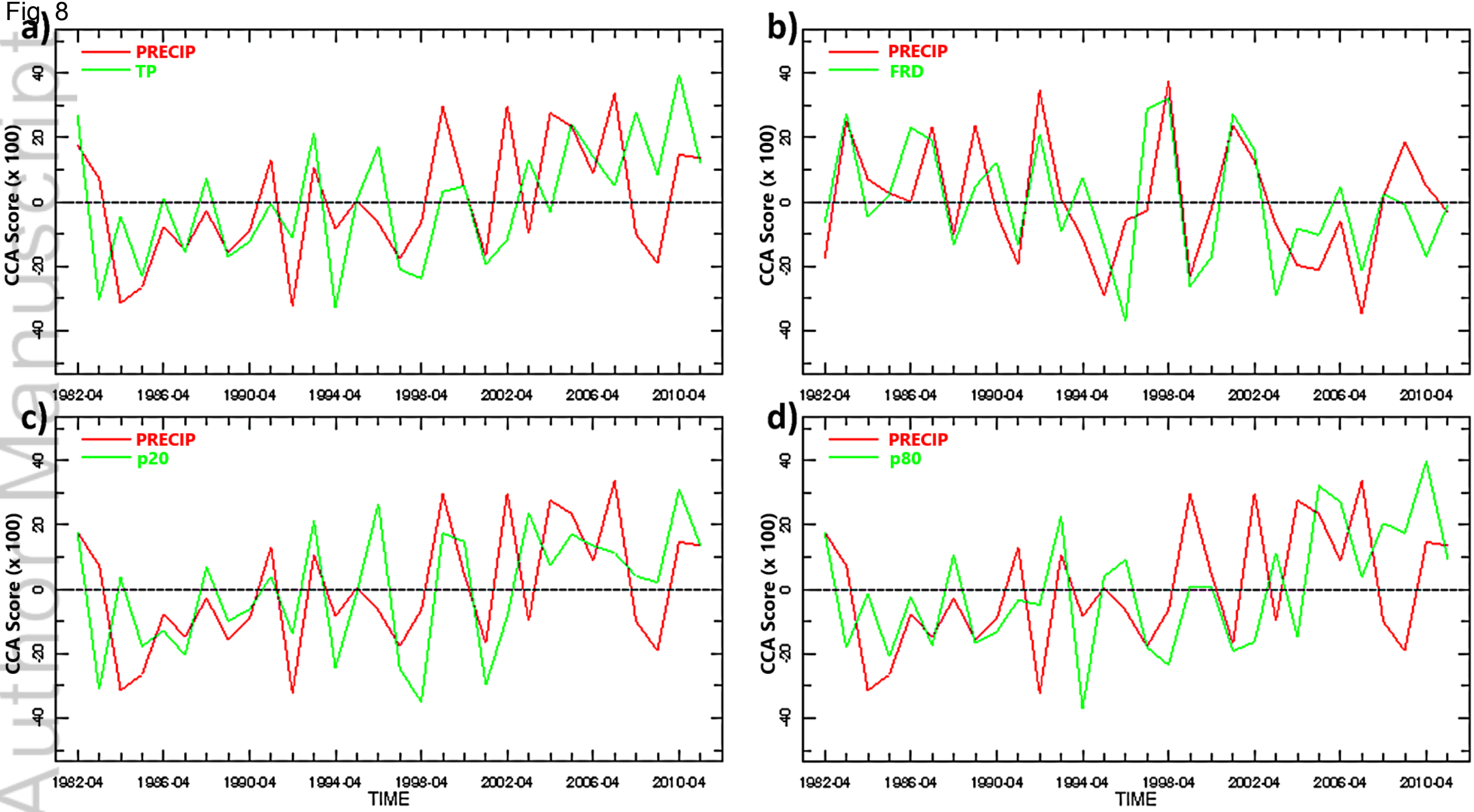

Improved seasonal prediction skill of rainfall for the *Primera* season in Central America

Eric J. Alfaro[1,2,3,], Xandre Chourio[4], Ángel G. Muñoz[5,6], Simon J. Mason[6]*

1- Center for Geophysical Research, University of Costa Rica

2- School of Physics, University of Costa Rica

3- Center for Research in Marine Sciences and Limnology, University of Costa Rica

4- Observatorio Latinoamericano de Eventos Extraordinarios (OLE^2). Centro de Modelado Científico (CMC). Universidad del Zulia. Maracaibo. Venezuela.

5- Atmospheric and Oceanic Sciences (AOS) and NOAA's Geophysical Fluid Dynamics Laboratory (GFDL). Princeton University. Princeton. USA.

6- International Research Institute for Climate and Society (IRI). The Earth Institute of Columbia University. New York. USA.

*** Corresponding author address:**

Escuela de Fisica, 11501, 2060-Ciudad Universitaria Rodrigo Facio, Universidad de Costa Rica, San Jose, Costa Rica.

tel: +506 2511-5096**, fax:** +506 2234-2703**, email:** erick.alfaro@ucr.ac.cr

Graphical Table of Contents

In Central America, outlooks of May-June season are important because drier seasons tend to be associated with late onsets of the rainy season. The region is at its wettest in the boreal late spring-early autumn, mainly because the formation of mesoscale convective systems like the one shown in the image. For that reason, a Model Output Statistics (MOS) technique is implemented for May-June prediction, using a combination of low-level winds and convective available potential energy (CAPE) over the region.

Contents